The Direct Synthesis of H_2O_2 Using TS-1 Supported Catalysts.

Richard J. Lewis,[a] Kenji Ueura,[b] Yukimasa Fukuta,[b] Simon J. Freakley,[a,c] Liqun Kang,[d] Ryan Wang,[d] Qian He,[a] Jennifer. K. Edwards,[a] David J. Morgan,[a,e] Yasushi Yamamoto[b] and Graham J. Hutchings*[a]

Abstract: In this study we show that using gold palladium nanoparticles supported on a commercial titanium silicate (TS-1) prepared using a wet co-impregnation method it is possible to produce hydrogen peroxide from molecular H_2 and O_2 via the direct synthesis reaction. The effect of Au: Pd ratio and calcination temperature is evaluated as well as the role of platinum addition to the AuPd supported catalysts. The effect of platinum addition to gold-palladium nanoparticles is observed to result in a significant improvement in catalytic activity and selectivity to hydrogen peroxide with detailed characterisation indicating this is a result of selectively tuning the ratio of palladium oxidation states.

Introduction.

Hydrogen peroxide (H_2O_2) is a powerful, environmentally friendly industrial oxidant, with a particularly high active oxygen content (47.1 %), second only to molecular O_2. In comparison to other commonly utilised oxidising agents such as tBuOOH, NaClO and permanganate, which all produce hazardous by-products that require downstream separation from product stream, H_2O_2 produces only H_2O as a by-product. Although finding increasing use in the treatment of industrial waste streams, due to increasing legislation preventing the use of chloride containing oxidants, H_2O_2 is primarily utilised in the paper / pulp bleaching and textile industries as well as in the chemical synthesis sector. Currently global demand for H_2O_2 is growing at a rate of 4% per annum[1] and is expected to exceed 5.5 million tons by 2020.[2] This demand is driven primarily from the chemical synthesis sector with H_2O_2 finding application in the production of propylene oxide[3-9] (via the integrated HPPO process) and cyclohexanone oxime[10-12] (via cyclohexanone ammoximation) which are key intermediates for the production of polyurethane and Nylon-6 respectively. In recent years Solvay, a technology leader with an extended product portfolio in H_2O_2, have doubled their H_2O_2 production capacity to meet growing demand for propylene oxide.[13]   Other significant applications of H_2O_2 are found in, but are by no means limited to, alkene epoxidation,[14-16] organo-sulphur oxidation,[17-19] aromatic side chain oxidation[20,21] and ketone oxidation.[22-25]

Currently the vast majority (95%) of global demand for H_2O_2 is met via the anthraquinone oxidation (AO) process, first developed by Riedl and Pfleiderer of BASF in 1939.[26] The AO process offers extremely high efficiency, producing H_2O_2 concentrations in excess of 70 wt.% through numerous distillation steps. However, there are some concerns around its carbon efficiency, in particular with the need to continually replenish the anthraquinone H_2 carrier molecule, which is deactivated through unselective hydrogenation.[27] In addition, the high infrastructure costs and the overall complexity of the AO process (in particular the choice of solvent system) prohibits production of H_2O_2 at point of use and so H_2O_2 is often transported at concentrations greatly exceeding that required by the end user, with costs associated with the dilution of H_2O_2 to appropriate concentrations, often between 5 and 10 wt.%. Furthermore, the instability of H_2O_2, at relatively mild temperatures, requires the use of acidic stabilising agents to prevent its decomposition to H_2O.[28-30] The use of such stabilising agents can result in a decrease in reactor lifetime, through corrosion, and pass on significant costs to the end user who must ensure they are removed from product streams in order to prevent the build-up of impurities.

The shortcomings of the anthraquinone process can be overcome via the direct synthesis of H_2O_2 from H_2 and O_2, outlined in Figure 1, which provides a greener, more atom efficient process for H_2O_2 generation and has the potential to be adopted at point of use. In particular, Pd-based catalysts have been demonstrated to offer high activity towards the direct synthesis of H_2O_2.[31-34] However, catalytic selectivity is often a concern and requires the use of halide and strong acid additives to inhibit H_2O_2 degradation and the production of H_2O via decomposition and hydrogenation pathways,[35-37] both of which are more thermodynamically favourable than the formation of H_2O_2

.

[a] Dr. R. Lewis, Dr. S. Freakley, Dr. Q. He, Dr. J. Edwards, Dr. D. Morgan and Prof. G. Hutchings.
Cardiff Catalysis Institute, School of Chemistry, Cardiff University, Main Building, Park Place, Cardiff, CF10 3AT, United Kingdom
E-mail: Hutch@cardiff.ac.uk
[b] Mr. K. Ueura, Dr. Y. Fukuta and Mr. Y. Yamamoto
UBE Industries,1978-5, Kogushi, Ube, Yamaguchi 755-8633, Japan
[c] Dr. S. Freakley, Department of Chemistry, University of Bath, Claverton Down, Bath BA2 7AY, United Kingdom.

[d] Mr. L Kang, Dr. R. Wang
Department of Chemical Engineering, University College London, Roberts Building, Torrington Place, London WC1E 7JE, United Kingdom.
[e] Dr. D. Morgan
HarwellXPS, Research Complex at Harwell (RCaH), Didcot, OX11 0FA, United Kingdom.
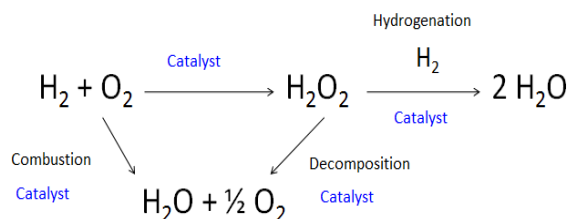
Figure 1. Reaction pathways associated with the direct synthesis of H_2O_2 from H_2 and O_2.

Building on the work of Landon et al.[38] and Haruta and co-workers,[39] Edwards et al.[40] were the first to demonstrate that high selectivity towards H_2O_2 can be achieved through combination of Pd with Au, with the development of a Au core-PdO shell often reported as a key factor in the enhancement of catalytic selectivity.[41,42] Indeed, these bimetallic Au-Pd catalysts have received significant attention by both experimentalists[43-46] and theoreticians[47,48] with a combination of electronic, structural and isolation effects likely to be responsible for the synergy observed in Au-Pd systems.

Numerous studies have investigated the modification of supported Pd nanoparticles through the addition of other precious metals such as Ag,[49,50] Rh,[51] Ru,[52] Ir[53] and Pt.[54-57] With Deguchi et al.[53] recently reporting that dramatic enhancements in catalytic activity can be achieved through the introduction of very low concentrations of Pt into a Pd-polyvinylpyrrolidone colloid, with the high H_2 activating abilities of Pt suggested as the cause for a doubling in H_2O_2 synthesis rates. This is in keeping with the work of Bernardotto et al.[58] who report that the introduction of a small amount of Pt into a supported Pd catalyst (Pd: Pt ratio = 13) leads to a significant enhancement in activity towards H_2O_2 synthesis in comparison to the analogous mono-metallic Pd catalyst. This has been attributed to a change in Pd nanoparticle morphology[58] and the stabilisation of the oxidised Pd surface.[55,59] More recently Quon et al.[60] have combined both an experimental and theoretical approach to investigate the role of Pt incorporation into a Pd catalyst. They report that the addition of low concentrations of Pt promote the hydrogenation of molecular O_2, leading to the production of H_2O_2 and inhibit the dissociation of H_2O_2, with a doubling of H_2O_2 production rate and a similar increase in H_2 selectivity. We have previously investigated the addition of Pt to AuPd supported nanoparticles and demonstrated an enhancement in catalytic selectivity towards the direct synthesis of H_2O_2 via the inhibition of the subsequent hydrogenation/decomposition pathways, when supported on CeO_2[61] and TiO_2.[62]

Since its first development by EniChem[63] the MFI-type zeolite titanium silicate-1 (TS-1) has widely been reported to offer high selectivity and efficiency in oxidation reactions when used alongside pre-formed H_2O_2. In particular TS-1 has been reported to show excellent activity for aromatic hydroxylation,[64,65] alkane oxidation[66] and alkene epoxidation.[67] With the combination of the hydrophobicity of the silicate lattice and the high coordination ability of the framework Ti^{IV} sites key to the unique catalytic properties observed for TS-1. In particular the catalytic conversion of propylene to propylene oxide is a pertinent example of a major industrial process that utilises TS-1, with over 1.2 Mt of propylene oxide produced annually, and the vast majority utilised in the production of polyurethane via the HPPO process. Furthermore, a growing interest has been placed on Au[68,69] and Au-Pd[70,71] nanoparticles supported on TS-1 for the *in situ* generation of H_2O_2 for a variety of selective oxidation reactions. We have previously investigated the role of zeolites such as TS-1, HZSM-5 and zeolite-Y as supports for precious metals in the direct synthesis of H_2O_2[72,73] as well as CO oxidation,[74] with H_2O_2 productivities for the zeolite supported catalysts much greater than the analogous catalysts supported on common oxide supports including TiO_2,[75] Al_2O_3[76] and SiO_2[77] likley due to their strong acid characters.

Building on these findings we now investigate the use of a commercial TS-1 as a support for AuPdPt nanoparticles for H_2O_2 synthesis from molecular H_2 and O_2.Results and Discussion.

Our initial screening of TS-1 supported monometallic (Au, Pd, Pt) and bimetallic (Au-Pd, Pd-Pt, Pt-Au) catalysts for the direct synthesis of H_2O_2 and its subsequent degradation (comprising over-hydrogenation and decomposition) are shown in Table 1. It was observed that the monometallic 5% Au / TS-1 catalyst has limited activity towards H_2O_2 synthesis (2 $mol_{H2O2}kg_{cat}^{-1}h^{-1}$), in comparison the 5% Pd / TS-1 catalyst was shown to have much greater activity towards both H_2O_2 synthesis (131 $mol_{H2O2}kg_{cat}^{-1}h^{-1}$) and the subsequent degradation of H_2O_2 (459 $mol_{H2O2}kg_{cat}^{-1}h^{-1}$). This is consistent with many previous studies investigating Au-Pd nanoparticles supported on various oxide support materials, with the Pd supported Al_2O_3 (200 $mol_{H2O2}kg_{cat}^{-1}h^{-1}$)76 and SiO_2 (488 $mol_{H2O2}kg_{cat}^{-1}h^{-1}$)77 catalysts demonstrating high H_2O_2 degradation values. In keeping with many previous studies into co-impregnation of Au and Pd to produce a bimetallic catalyst we observe enhanced catalytic activity when both Au and Pd are immobilised onto the same support with the activity of the bi-metallic 2.5% Au-2.5% Pd / TS-1 catalyst (100 $mol_{H2O2}kg_{cat}^{-1}h^{-1}$), greater than that observed over a physical mixture of the mono-metallic catalysts with an analogous metal loading (87 $mol_{H2O2}kg_{cat}^{-1}h^{-1}$). However, catalytic activity of the bi-metallic AuPd / TS-1 catalyst does not supersede that of the mono-metallic Pd supported catalyst, which had previously been reported on a range of oxide supports, including TiO_2,[75] MgO[78] and Al_2O_3,[76] and this is attributed to a lack of complete alloying and only partial formation of the Au-core-PdO shell nanoparticle morphology often adopted on oxide supports. This is in keeping with our previous work investigating the catalytic activity of Au-Pd catalysts supported on SiO_2[77] and highlights how the choice of support can enhance catalytic activity toward H_2O_2 formation. Indeed it has previously been reported that supports such as SiO_2 that have low isoelectric points yield catalysts that are

highly selective towards H_2O_2,[78] with Drago et al. investigating the acidity of TS-1, finding it to be similar to that of SiO_2.[79] It should also be noted that the activity of the 2.5% Au- 2.5% Pd / TS-1 catalyst is significantly greater than that of the well-studied 2.5% Au- 2.5% Pd / TiO_2 catalyst[75] and the analogous 2.5% Au- 2.5% Pd / SiO_2.[77]

In addition, it is observed that the incorporation of Au into a TS-1 supported Pt catalyst can result in a remarkable synergistic enhancement in catalytic activity towards the synthesis of H_2O_2 with the activity of the bimetallic 2.5% Au- 2.5% Pt / TS-1 catalyst (98 $mol_{H2O2}kg_{cat}^{-1}h^{-1}$) much greater than that of the 5% Au / TS-1 or 5% Pt / TS-1 catalysts. Indeed as reported previously for the 2.5% Au- 2.5% Pd / TS-1 catalyst the co-impregnation of Au and Pt onto the same support surface is observed to offer enhanced activity compared to that of a physical mixture of the two mono-metallic analogues (13 $mol_{H2O2}kg_{cat}^{-1}h^{-1}$) and demonstrates the beneficial role of Au addition to precious metals which are active towards H_2O_2 synthesis.

Table. 1. Catalytic activity of TS-1 supported monometallic and bimetallic catalysts towards H_2O_2 synthesis and its subsequent degradation.

Catalyst	Productivity / $mol_{H2O2}kg_{cat}^{-1}h^{-1}$ [a]	H_2O_2 Degradation / $mol_{H2O2}kg_{cat}^{-1}h^{-1}$ [b]
5% Au / TS-1	2	6
5% Pd / TS-1	131	459
5% Pt / TS-1	29	119
2.5% Au – 2.5% Pd / TS-1	100	316
2.5 % Au / TS-1 + 2.5% Pd / TS-1	87	210
2.5% Au – 2.5% Pt / TS-1	98	255
2.5 % Au / TS-1 + 2.5% Pt / TS-1	13	59
2.5% Pd – 2.5% Pt / TS-1	114	286
TS-1	0	0
2.5% Au – 2.5% Pd / TiO_2	64	235
TiO_2	0	0
2.5% Au – 2.5% Pd / SiO_2	74	488
SiO_2	0	158

[a] **H_2O_2 direct synthesis reaction conditions:** Catalyst (0.01g), H_2O (2.9g), MeOH (5.6g), 5% H_2 / CO_2 (420 psi), 25% O_2 / CO_2 (160 psi), 0.5 h, 2 °C 1200 rpm.
[b] **H_2O_2 degradation reaction conditions:** Catalyst (0.01g), H_2O_2 (50 wt.% 0.68 g) H_2O (2.22g), MeOH (5.6g), 5% H_2 / CO_2 (420 psi), 0.5 h, 2 °C 1200 rpm.

Investigation of the calcined 2.5% Au - 2.5% Pd /TS-1 catalyst by Fourier-transform infrared spectroscopy (FTIR) (Figure S.1) reveals no discernible change in the observed positions of the absorption bands compared to a standard unmodified material suggesting that the structure of TS-1 remains unchanged during catalysts preparation. Indeed, no change in the structure of the titanosilicate can be observed upon impregnation of Au and Pd and subsequent calcination at temperatures up to 800 °C. This is unsurprising given the high thermal stability of TS-1.[79]It is possible to observe four distinct infrared bands in the FTIR spectra of AuPd / TS-1,with bands at 800 cm^{-1} and 1100 cm^{-1} assigned to lattice modes associated with internal linkages in tetrahedral SiO_4, the band at 990 cm^{-1} assigned to stretching vibrations of SiO_4 tetrahedra bound to Ti atoms as Si-O-Ti linkages and the band at 1240 cm^{-1} assigned to tetrahedral Ti present in the TS-1 framework.[80] The

details of the textural properties of TS-1 and the supported AuPd catalyst are summarised in Table 2 (Figure S.2). It can be seen that upon immobilisation of metal nanoparticles total surface area and total pore volume decreases slightly from 421 m^2g^{-1} and 0.216 cm^3g^{-1} for the as received TS-1 sample to 384 m^2g^{-1} and 0.139 cm^3g^{-1} upon co-impregnation of the precious metals, followed by calcination. We ascribe this decrease to result from the deposition of metal nanoparticles inside the zeolitic pore structure.

Table 2. Summary of porosity and surface area of TS-1 supported catalysts.

Catalyst	Surface area[a] / m^2g^{-1}	$V_{Micropore}$ / cm^3g^{-1}
TS-1	421	0.212
2.5%Au-2.5%Pd/TS-1 (Dried)*	410	0.147
2.5%Au-2.5%Pd/TS-1 (400 °C, 3 h air)	384	0.139

* Catalyst dried only static air, 110 °C, 16 h.
[a] Surface area determined from nitrogen adsorption measurements using the BET equation.

Analysis by XRD (Figure S.3) reveals that, as with FTIR analysis, there is no apparent change in the structure of the TS-1 support, upon the impregnation of precious metals and subsequent calcination at 400 °C, according to the main reflection peaks associated with TS-1 (θ = 23.1°, 23.9°, 24.4° and 24.5°), with these reflections often cited in literature to demonstrate the typical MFI structure.[81] In particular the single reflection at 24.2° indicates the orthorhombic symmetry of TS-1.[63] However, it should be noted that our analysis by XRD does not account for the reflections below θ = 10°.[82] Upon impregnation of the metals and calcination at 400 - 800 °C reflections associated with Au (θ = 38°, 44° and 70°) are observed, suggesting Au is present as large, poorly dispersed, nanoparticles, regardless of calcination temperature. This is corroborated via EDX analysis (Figure S.4.), which reveals the presence of large Au nanoparticles. Conversely, no reflections associated with Pd can be observed upon calcination at 400 °C. However, upon calcination at 600 °C reflections associated with PdO (θ = 34°) are observed, suggesting the agglomeration of metal nanoparticles at elevated temperatures. Further analysis by transmission electron microscopy (TEM) corroborates this finding with a significant increase in mean particle size observed with increasing calcination temperature, from 6.4 nm to 30.5 nm as calcination temperature increases from 400 to 800 °C (Figure S.5). However it should be noted that the 2.5% Au- 2.5% Pd / TS-1 catalyst calcined at 400 °C shows a relatively tight mean particle size, with no nanoparticles observed in excess of 50 nm, which is atypical of catalysts prepared by a wet-impregnation methodology and is ascribed in part to the large surface area of the TS-1 support.

Investigation of the dried only catalyst by X-ray photoelectron spectroscopy (XPS) reveals a surface Pd:Au ratio of 0.5, suggesting, on average, a significant surface enrichment by Au in the uncalcined sample. In contrast upon calcination at 400 °C a significant

increase in Pd : Au ratio is observed (Pd:Au = 19) consistent with the development of a Au-core PdO shell morphology with increasing calcination temperature and identical to that reported previously for the analogous 2.5% Au-2.5% Pd / TiO$_2$ catalyst.[75] As calcination temperature increases beyond 400 °C the surface atomic ratio of Au: Pd decreases significantly from 19 to 2.6, (Table S.1) possibly as a result of Au surface migration or particle agglomeration as indicated by XRD and TEM analysis.

Investigation into the effect of calcination temperature on catalytic activity towards H$_2$O$_2$ formation and its subsequent degradation can be seen in Table 3. A direct correlation is drawn between calcination temperature and catalytic activity; with increasing calcination temperature catalyst activity towards both H$_2$O$_2$ synthesis and degradation decreases. Evaluation of catalyst activity upon re-use revealed that the dried only catalyst retained approximately 58 % of its initial H$_2$O$_2$ synthesis activity. This loss in catalytic activity is attributed to leaching of active metals from the support with significant loss of Au and Pd observed via MP-AES analysis for the dried only catalyst (Table S.2). This leaching is observed to decrease with increasing calcination temperature with similar findings previously reported for 2.5% Au- 2.5% Pd / TiO$_2$, prepared via a similar methodology.[75] When calcined at 400 °C catalytic activity decreased from 152 mol$_{H2O2}$kg$_{cat}$$^{-1}$h^{-1} for the dried only sample to 100 mol$_{H2O2}$kg$_{cat}$$^{-1}$h^{-1} but crucially remained stable upon second use, with minimal leaching of Au and Pd observed. As discussed above a decrease in catalytic activity is observed to correlate with an increase in mean particle size as calcination temperature increases and this is in keeping with previous findings in the literature.[83]

Table 3. The effect of calcination temperature on the catalytic activity of 2.5% Au – 2.5% Pd / TS-1 towards H$_2$O$_2$ synthesis and its subsequent degradation.

Calcination temperature / °C	Initial Productivity / mol$_{H2O2}$kg$_{cat}$$^{-1}h^{-1 (a)}$	Re-use Productivity / mol$_{H2O2}$kg$_{cat}$$^{-1}h^{-1 (a)}$	H$_2$O$_2$ Degradation / mol$_{H2O2}$kg$_{cat}$$^{-1}h^{-1 (b)}$
Dried Only*	152	89	413
300	128	98	392
400	100	100	316
600	35	35	181
800	30	30	117

[a)]**H$_2$O$_2$ direct synthesis reaction conditions:** Catalyst (0.01g), H$_2$O (2.9g), MeOH (5.6g), 5% H$_2$ / CO$_2$ (420 psi), 25% O$_2$ / CO$_2$ (160 psi), 0.5 h, 2 °C 1200 rpm.[b)]**H$_2$O$_2$ degradation reaction conditions:** Catalyst (0.01g), H$_2$O$_2$ (50 wt.% 0.68 g) H$_2$O (2.22g), MeOH (5.6g), 5% H$_2$ / CO$_2$ (420 psi), 0.5 h, 2 °C 1200 rpm.
* Catalyst dried only static air, 110 °C, 16 h.

Further investigation into the effect of Au : Pd ratio on H$_2$O$_2$ formation and degradation can be seen in Figure 2. As previously reported for an analogous SiO$_2$ catalyst[77] activity towards H$_2$O$_2$ synthesis correlates well with total Pd content, possibly due to incomplete formation of the Au-core-PdO shell morphology often observed on oxide supports. As with activity towards H$_2$O$_2$ synthesis, catalytic degradation activity is also directly related to Pd content, with the 5% Au / TS-1 catalyst reported to have a minimal degradation activity (6 mol$_{H2O2}$kg$_{cat}$$^{-1}$h^{-1}), while the analogous Pd catalyst is observed to offer much greater degradation activity (459 mol$_{H2O2}$kg$_{cat}$$^{-1}$h^{-1}), similar to that previously reported for the analogous SiO$_2$ supported catalyst.[77] Analysis by

both XRD (Figure S.6) and EDX (Figure S.4) indicates the presence of poorly dispersed Au nanoparticles regardless of Au: Pd ratio, with XRD reflections for Au (θ= 38, 44 and 70°) observed in all samples.
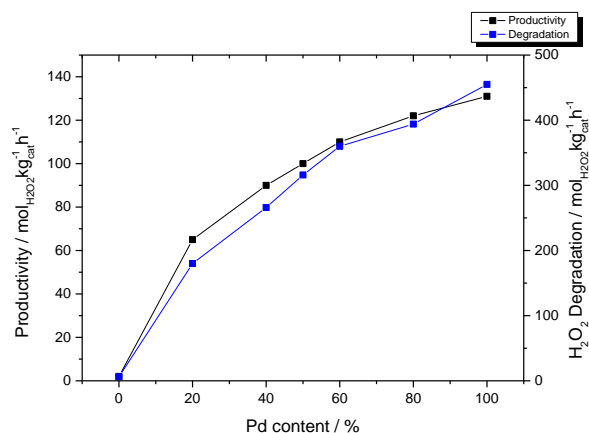

Figure 2. The effect of Au: Pd (wt/wt) ratio on catalytic activity of AuPd / TS-1 towards the direct synthesis and degradation of H$_2$O$_2$. **H$_2$O$_2$ direct synthesis reaction conditions:** Catalyst (0.01g), H$_2$O (2.9g), MeOH (5.6g), 5% H$_2$ / CO$_2$ (420 psi), 25% O$_2$ / CO$_2$ (160 psi), 0.5 h, 2 °C 1200 rpm. **H$_2$O$_2$ degradation reaction conditions:** Catalyst (0.01g), H$_2$O$_2$ (50 wt.% 0.68 g) H$_2$O (2.22g), MeOH (5.6g), 5% H$_2$ / CO$_2$ (420 psi), 0.5 h, 2 °C 1200 rpm.

Our previous studies have reported the activity of Pt containing Au-Pd supported catalysts towards the direct synthesis of H$_2$O$_2$,[61,62] Building on our initial findings and in an attempt to improve catalytic selectivity, we investigated the effect of Pt addition to 2.5% Au- 2.5% Pd / TS-1 on catalytic activity towards H$_2$O$_2$ synthesis and its subsequent degradation, with the results shown in Figure 3. As can be observed, the addition of a small amount of Pt (0.2 %) to a supported AuPd/TS-1 catalyst reduces the extent of H$_2$O$_2$ degradation significantly from 316 mol$_{H2O2}$kg$_{cat}$$^{-1}$h^{-1} for the 2.5% Au- 2.5% Pd / TS-1 catalyst, to 93 mol$_{H2O2}$kg$_{cat}$$^{-1}$h^{-1} for the 2.4% Au – 2.4% Pd -0.2% Pt / TS-1 catalyst. This corresponds with an increase in the rate of H$_2$O$_2$ synthesis, from 100 to 167 mol$_{H2O2}$kg$_{cat}$$^{-1}$h^{-1}. However, further addition of Pt results in an increase in degradation activity, with this metric rising to a maxima of 247 mol$_{H2O2}$kg$_{cat}$$^{-1}$h^{-1} for the 2% Au-2%Pd-f 1% Pt/ TS-1 catalyst. A corresponding decrease in H$_2$O$_2$ synthesis rate is observed (69 mol$_{H2O2}$kg$_{cat}$$^{-1}$h^{-1}) and this is in keeping with our previous investigations into the effect of Pt introduction into Au-Pd supported on CeO$_2$ [61] and TiO$_2$.[62]
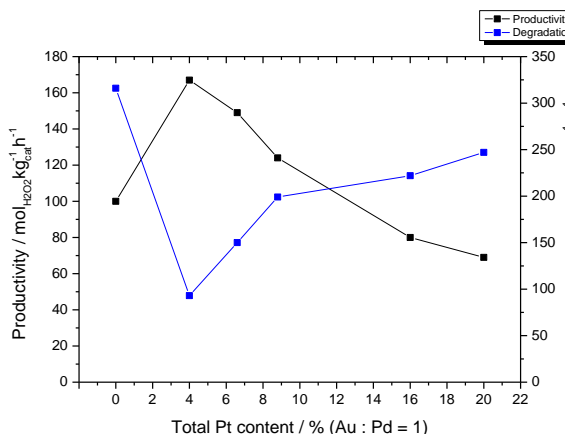
Figure 3. The effect of Pt incorporation into AuPd / TS-1 on catalytic activity towards the direct synthesis and degradation of H_2O_2. **H_2O_2 direct synthesis reaction conditions:** Catalyst (0.01g), H_2O (2.9g), MeOH (5.6g), 5% H_2 / CO_2 (420 psi), 25% O_2 / CO_2 (160 psi), 0.5 h, 2 ^{O}C 1200 rpm. **H_2O_2 degradation reaction conditions:** Catalyst (0.01g), H_2O_2 (50 wt.% 0.68 g) H_2O (2.22g), MeOH (5.6g), 5% H_2 / CO_2 (420 psi), 0.5 h, 2 ^{O}C 1200 rpm.

Investigation of the AuPdPt / TS-1 catalyst series by XRD is shown in Figure S.7, as with the bimetallic AuPd / TS-1 catalysts no reflections associated with PdO are observed, in comparison reflections associated with Au can be observed in all Au containing samples (θ = 38 ^{o}, 44 ^{o}) and potentially indicates the poor dispersion of Au on the support. This is in keeping with our analysis of the 2.4% Au – 2.4% Pd -0.2% Pt / TS-1 catalyst by Scanning Transmission Electron Microscopy (STEM) coupled with X-ray Energy Dispersive Spectroscopy (X-EDS) as seen in Figure 4 (STEM-ADF and corresponding X-EDS seen in Figure S.8) which reveals that metal nanoparticles immobilised on the titanosilicate surface consist of a combination of large (> 20 nm) Au-rich nanoparticles, which also contain Pd and Pt. In addition smaller (< 10 nm) nanoparticles are observed that contain both Au and Pd in similar quantities, while there also exists Pd-rich clusters in the range of 2 nm.
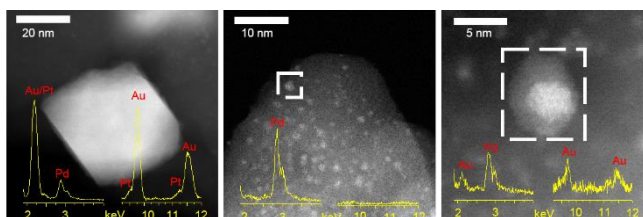

Figure 4. HAADF images of 2.4% Au – 2.4% Pd – 0.2% Pt / TS-1 calcined sample and corresponding EDS spectra. Note the presence of large Au-rich, Pd-rich and Au-Pd alloy particles.

Further analysis by XPS can be seen in Table 4, as with the 2.5% Au- 2.5% Pd / TS-1 catalyst the observed Pd :Au surface atomic ratios for the AuPdPt / TS-1 catalysts are much higher than those calculated from the nominal compositions. It is observed that upon the introduction of a small amount of Pt the Pd: Au surface atomic ratio increases marginally from 19 for the 2.5% Au – 2.5% Pd / TS-1 catalyst to 22 for the 2.4% Au – 2.4% Pd -0.2% Pt / TS-1 catalyst. Although this may be

a result of a minor enhancement of the Au-core PdO-shell morphology, often observed on oxide supported catalysts, analysis by EDS (Figure 3) does not provide any evidence for a Pd-rich outer later. Further introduction of Pt results in a minor decrease in the Pd: Au ratio, again this is in keeping with our previous studies.[61,62] Perhaps more interestingly the addition of Pt is observed to significantly enhance Pd^0 content, with the Pd^{2+} :Pd^0 ratio increasing significantly from 1 (all Pd present as Pd^{2+})for the 2.5% Au-2.5% Pd / TiO_2 catalyst to 0.55 with the incorporation of a small amount of Pt, with further Pt addition enhancing Pd^0 content, with the low selectivity of Pd^0 towards H_2O_2 well reported in the literature.[51] However Ouyang et al.[84] have reported the enhanced selectivity and activity of supported Pd catalysts containing Pd^0-Pd^{2+} ensembles in comparison to those catalysts with predominance of either Pd oxidation state. With this ascribed to the propensity of H_2 to dissociate on Pd^0 and the enhanced stability of O_2 on PdO surfaces, with the maintenance of the O-O bond required for the formation of H_2O_2 over H_2O. It is therefore possible to relate the enhanced catalytic performance of the 2.4% Au – 2.4% Pd -0.2% Pt / TS-1 catalyst due to the development of these Pd domains of mixed oxidation state. While the increased degradation rates observed at higher Pt loadings results from a significant increase in Pd^0 content.

Table 4. Effect of Pt incorporation on Au: Pd atomic ratio of supported Au- Pd / TS-1 catalysts as determined by XPS analysis.

Catalyst	Pd: Au*	Pd^{2+} :Pd^0
2.5% Au – 2.5% Pd / TS-1	19	1.00
2.4 % Au – 2.4% Pd -0.2% Pt / TS-1	22	0.55
2.35% Au – 2.35% Pd -0.3% Pt / TS-1	18	0.36
2.28% Au – 2.28% Pd -0.44% Pt / TS-1	17	0.35
2 % Au – 2% Pd – 1% Pt / TS-1	n.d.	n.d.

All catalysts calcined 400 ^{o}C, 3 h, 20 ^{o}Cmin^{-1}, static air.
n.d: not determined. * Expected value = 1.9

Particle size derived from transmission electron microscopy, seen in Table 5 and Figure S.9, reveals that mean particle size is similar for the 2.5% Au – 2.5% Pd / TS-1 (6.4 nm) and 2.4% Au – 2.4% Pd -0.2% Pt / TS-1 (7.2 nm) catalysts despite the distinct contrast in catalytic performance. The observation that mean particle size increases only slightly upon addition of small quantities of Pt suggests that the enhancement in catalytic synthesis activity cannot be associated with metal dispersion. With further addition of Pt mean particle size decreases significantly to 2.6 nm for the 2% Au– 2% Pd -1% Pt / TS-1 catalyst, with a corresponding decrease in catalytic selectivity towards H_2O_2. We have previously reported a correlation between mean nanoparticle size and catalytic selectivity towards H_2O_2 for AuPd catalysts supported on TiO_2 with larger AuPd nanoparticles displaying a higher selectivity towards H_2O_2.[85] It is therefore possible to correlate this significant decrease in mean particle size with a loss of catalytic selectivity.

Table 5. Particle size of AuPdPt / TS-1 catalysts as determined by TEM.

Catalyst	Particle size / nm (Standard deviation)
2.5% Au – 2.5% Pd / TS-1	6.4 (3.6)
2.4% Au – 2.4% Pd -0.2% Pt / TS-1	7.2 (4.27)
2% Au – 2% Pd – 1% Pt / TS-1	2.6 (0.99)

All catalysts calcined 400 ˚C, 3 h, 20 ˚Cmin^{-1}, static air.

For any heterogeneous catalyst operating in a three-phase system the possibility of the leaching of the active phase and resulting homogeneous contribution towards activity or deactivation of the catalyst is of great concern, with the activity of homogeneous Pd towards the formation of H_2O_2 previously reported by Dissanayke and Lunsford.[86] We have already established the need for the use of an appropriate heat treatment procedure to impart catalyst stability, with a minimum calcination temperature of 400 °C required to produce a stable AuPd / TS-1 catalyst (Table 2). Further investigation into the catalytic stability of the optimal 2.4% Au- 2.4% Pd- 0.2% Pt / TS-1 catalyst exposed to an identical heat treatment regime can be seen in Figure 5.
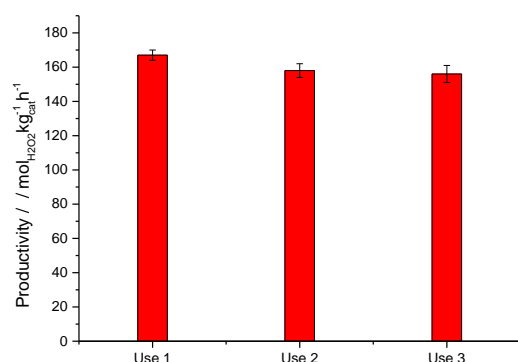

Figure 5. Catalyst stability of 2.4% Au- 2.4% Pd- 0.2% Pt / TS-1 catalyst towards the direct synthesis and degradation of H_2O_2.
H_2O_2 direct synthesis reaction conditions: Catalyst (0.01g), H_2O (2.9g), MeOH (5.6g), 5% H_2 / CO_2 (420 psi), 25% O_2 / CO_2 (160 psi), 0.5 h, 2 °C 1200 rpm.

As can be seen catalytic activity is observed to decrease marginally with re-use, from 167 to 156 $mol_{H2O2}kg_{cat}^{-1}h^{-1}$, with this loss ascribed to the leaching of Pd and Pt over the first two uses, as determined by MP-AES analysis of the digested post-reaction catalyst (Table S.3). Total leaching of Pd and Pt over the first two uses is observed to be 2.6 and 2.2 % of the total individual elemental loading respectively. It should be noted that after two uses no further loss of either Pd or Pt is detected. Interestingly no loss of Au is observed, which is keeping with our previous work investigating the stability of 2.5% Au- 2.5% Pd/ TiO_2.[75]

Conclusions.

We have investigated the activity of TS-1 supported AuPd and AuPdPt catalysts prepared by a conventional co-impregnation methodology for the direct synthesis of H_2O_2. Furthermore, we establish a means of imparting catalyst stability through choice of appropriate heat treatment while maintaining the MFI structure of the zeolite. Through the introduction of small concentrations of Pt into a supported AuPd/TS-1 catalyst it is possible to significantly enhance catalytic selectivity towards H_2O_2. The addition of Pt to AuPd / TS-1 in a Au:Pd:Pt ratio of 1 : 1 : 0.2 is shown to suppress catalytic activity towards H_2O_2 degradation, thus improving overall yields of H_2O_2. We ascribe this improvement in catalytic selectivity to the development of Pd domains of mixed oxidation state, well known for its high selectivity towards H_2O_2. We believe that these catalysts represent a promising system to explore the direct synthesis of H_2O_2.

Experimental Section.

Catalyst Preparation.
Au-Pd and Au-Pd-Pt / TS-1 catalysts have been prepared (on a weight metal basis) by wet co-impregnation of metal salts, based on methodology previously reported in the literature.[75] The procedure to produce 2 g of 2.4% Au – 2.4% Pd- 0.2% Pt / TS-1 is outlined below, with a similar methodology utilised for mono- and bi-metallic catalysts.

$PdCl_2$ (8.00 ml, 6 mgml^{-1}, Sigma Aldrich), $HAuCl_4.3H_2O$ solution (3.9184 ml, 12.25 mgml^{-1}, Strem Chemicals) and $H_2PtCl_6.6H_2O$ (0.4211 ml, 9.5 mg ml^{-1}, Sigma Aldrich) were placed in a 50 ml round bottom flask, with total volume fixed to 16 ml using H_2O (HPLC grade). The resulting mixture was heated to 65 °C in a thermostatically controlled oil bath with stirring (1000 rpm). Upon reaching 65 °C TS-1 (1.90 g, ACS Materials) was added over the course of 5 minutes. The resulting slurry was then heated to 85 °C for 16 h to allow for complete evaporation of water. The resulting solid material was ground prior to calcination in static air (400 °C, 3h, 20 °C min^{-1}).

Direct Synthesis of H_2O_2.
Hydrogen peroxide synthesis was evaluated using a Parr Instruments stainless steel autoclave with a nominal volume of 100 ml and a maximum working pressure of 14 MPa. To test each catalyst for H_2O_2 synthesis, the autoclave was charged with catalyst (0.01 g), solvent (5.6 g MeOH and 2.9 g H_2O). The charged autoclave was then purged three times with 5% H_2 / CO_2 (0.7 MPa) before filling with 5% H_2 / CO_2 to a pressure of 2.9 MPa, followed by the addition of 25 % O_2 / CO_2 (1.1 MPa). The temperature was then decreased to 2 °C followed by stirring (1200 rpm) of the reaction mixture for 0.5 h. The above reaction parameters represent the optimum conditions we have previously used for the synthesis of H_2O_2.[75] Our choice of reaction solvent has been previously been shown to be optimal for H_2O_2 synthesis, with the higher solubility of H_2 in MeOH compared to H_2O a key factor in achieving enhanced yields of H_2O_2.[87] H_2O_2 productivity was determined by titrating aliquots (approximately 0.5 g) of the final solution after reaction with acidified $Ce(SO_4)_2$ (0.01 M)

in the presence of ferroin indicator. Catalyst productivities are reported as $mol_{H2O2}kg_{cat}^{-1}h^{-1}$.

Catalyst Reusability in the Direct Synthesis of H_2O_2.
In order to determine catalyst reusability a similar procedure to that outlined above for the direct synthesis of H_2O_2 is followed utilising 50 mg of catalyst. Following the initial test the catalyst is recovered by filtration and dried (110 °C, 16 h, air), from the recovered catalyst sample 10 mg is used to conduct a H_2O_2 synthesis test as outlined above.

Degradation of H_2O_2.
Catalytic activity towards H_2O_2 degradation was determined in a manner similar to the direct synthesis activity of a catalyst. The autoclave was charged with MeOH (5.6 g), H_2O_2 (50 wt. % 0.69 g) HPLC standard H_2O (2.21 g) and catalyst (0.01 g), with the solvent composition equivalent to a 4 wt. % H_2O_2 solution. From the solution 2 aliquots of 0.05 g were removed and titrated with acidified $Ce(SO_4)_2$ solution using ferroin as an indicator to determine an accurate concentration of H_2O_2 at the start of the reaction. The autoclave was pressurised with 2.9 MPa 5 % H_2 / CO_2 and cooled to 2 °C. Upon reaching 2 °C the reaction mixture was stirred at 1200 rpm for 0.5 h. After the reaction was complete the catalyst was removed from the reaction solvents and as previously two aliquots (approximately 0.05 g) were titrated against an acidified $Ce(SO_4)_2$ solution using ferroin as an indicator. The degradation activity is reported as $mol_{H2O2}kg_{cat}^{-1}h^{-1}$.

Catalyst Characterisation.
Fourier-transform infrared spectroscopy (FTIR) was carried out with a Bruker Tensor 27 spectrometer fitted with a HgCdTe (MCT) detector and operated with OPUS software.

N_2 isotherms were collected on a Micromeritics 3Flex. Samples (ca. 0.020 g) were degassed (150 °C, 6 h) prior to analysis. Analyses were carried out at 77 K with P_0 measured continuously. Free space was measured post- analysis with He. Pore size analysis was carried out using Micromeritics 3Flex software, N_2-Cylindrical Pores- Oxide Surface DFT Model.

Investigation of the bulk structure of the crystalline materials was carried out using a (θ-θ) PANalytical X'pert Pro powder diffractometer using a Cu K_α radiation source, operating at 40 KeV and 40mA. Standard analysis was carried out using a 40 min run with a back filled sample, between 2θ values of 10 – 80°. Phase identification was carried out using the International Centre for Diffraction Data (ICDD).

X-ray photoelectron spectroscopy (XPS) analyses were made on a Kratos Axis Ultra DLD spectrometer. Samples were mounted using double-sided adhesive tape and binding energies were referenced to the C (1s) binding energy of adventitious carbon contamination that was taken to be 284.7 eV. Monochromatic AlK$_\alpha$ radiation was used for all measurements; an analyser pass energy of 160 eV was used for survey scans while 40 eV was employed for detailed regional scans. The intensities of the Au (4f), Pt (4f) and Pd (3d) features were used to derive the Pd / Pt and Au / Pt surface ratios.

Transmission electron microscopy (TEM) was performed on a JEOL JEM-2100 operating at 200 kV. Samples were prepared by dispersion in ethanol by sonication and deposited on 300 mesh copper grids coated with holey carbon film. Energy dispersive X-ray analysis (EDX) was performed using an Oxford Instruments X-Max^N 80 detector and the data analysed using the Aztec software.

Scanning Transmission Electron Microscopy (STEM) and X-ray Energy Dispersive Spectroscopy (X-EDS) data was taken using a JEOL JEM-ARM200CF microscope in Diamond Laboratory. The TEM specimen investigated was 2.4% Au – 2.4% Pd – 0.2% Pt / TS-1 prepared by co-impregnation of precious metals onto the titanosilicate support, calcined at 400 °C, 3 h, 20 °Cmin^{-1}, static air.

Metal leaching was quantified using microwave plasma - atomic emission spectroscopy (MP-AES). Post-reaction solid catalysts were digested (10 mg catalyst, 10 ml aqua-regia, 16 h) prior to analysis using an Agilent 4100 MP-AES.

[1] Y. Yi, L. Wang, G. Li, H. Guo, *Catal. Sci. Technol.* **2016**, *6*, 1593-1610.
[2] M. Seo, H. J. Kim, S. S. Han, K. Lee. *Catal. Surv. Asia,* **2017**, *21*, 1-12.
[3] M. Lin, C. Xia, B. Zhu, H. Li, X. Shu,. *Chem. Eng. J.* **2016**, *295*, 370-375.
[4] Y. Wang, H. Li, W. Liu, Y. Lin, X. Han, Z. Wang, *Trans. Tianjin Univ.* **2018**, *24*, 25-31.
[5] G.Blanco-Brieva, M. Capel-Sanchez, M.P. de Frutos, A. Padilla-Polo, J.M. Campos-Martin, J. L. G Fierro, *Ind. Eng. Chem. Res.* **2008**, *47*, 8011-8015.

[6] J. M. Campos-Martin, G. Blanco-Brieva, J. L. *Angew. Chem. Int. Ed.* **2006**, *45*, 6962-6984.

[7] S. B. Shin, D. Chadwick, *Ind. Eng. Chem. Res.* **2010**, *49*, 8125-8134.

[8] V. Russo, R. Tesser, E. Santacesaria, M. Di Serio, *Ind. Eng. Chem. Res.* **2013**, *52*, 1168-1178.

[9] G. Xiong, Y. Cao, Z. Guo, Q. Jia, Q. F. Tian, L. Liu, *Phys. Chem. Chem. Phys.* **2016**, *18*, 190-196.

[10] G. Liu, J. Wu, H. Luo, *Chin. J. Chem. Eng.* **2012**, *20*, 889-894.

[11] L. Xu, J. Ding, Y. Yang, P. Wu, *J. Catal.* **2014**, *309*, 1-10.

[12] L. Dal Pozzo, G. Fornasari, T. Monti, *Catal. Commun.* **2002**, *3*, 369-375.

[13] Solvay.com. (2019). *A Hydrogen Peroxide mega plant in Saudi Arabia to meet the world's needs for Polyurethane foams*. [online] Available at: https://www.solvay.com/en/article/hydrogen-peroxide-plant-saudi-arabia-polyurethane-foams [Accessed 10 Jan. 2019].

[14] C. Peng, X. H. Lu, X. T. Ma, Y. Shen, C. C. Wei, J. He, D. Zhou, Q. H. Xia, *J. Mol. Catal. A.* **2016**, *423*, 393-399.

[15] R. Fareghi-Alamdari, S. M. Hafshejani, H. Taghiyar, B. Yadollahi, M. R. Farsani, *Catal. Commun.* **2016**, *78*, 64-67.

[16] A. Rezaeifard, M. Jafarpour, R. Haddad, F. Feizpour, *Catal. Commun.* **2017**, *95*, 88-91.

[17] K. Kaczorowska, Z. Kolarska, K. Mitka, P. Kowalski, *Tetrahedron,* **2005**, *61*, 8315-8327.

[18] F.Gregori, I. Nobili, F. Bigi, R. Maggi, G. Predieri, G. Sartori, *J. Mol. Catal. A.,* **2008**, *286*, 124-127.

[19] M. Kirihara, J. Yamamoto, T. Noguchi, Y. Hirai, *Tetrahedron Lett.* **2009**, *50*, 1180-1183.

[20] K. Nomiya, K. Hashino, Y. Nemoto, M. Watanabe, *J. Mol. Catal. A.,* **2001**, *176*, 79-86.

[21] S. Peta, T. Zhang, V. Dubovoy, K. Koh, M. Hu, X. Wang, T. Asefa, *Mol. Catal.* **2018**, *444*, 34-41.

[22] Q, Ma, W. Xing, J. Xu, X. Peng, *Catal. Commun.* **2014**, *53*, 5-8.

[23] X. Cui, J. Shi, *Sci. China Mater.* **2016**, *59*, 675-700.

[24] H. Xu, J. Jiang, B. Yang, H. Wu, P. Wu, *Catal. Commun.* **2014**, *55*, 83-86.

[25] X. Li, R. Cao, Q. Lin, *Catal. Commun.* **2015**, *63*, 79-83.

[26] H. J. Riedl, G. Pfleiderer, (I. G. Farbenindustrie AG) US2158525A **1939**.

[27] C. Samanta, *Appl. Catal. A.* **2008**, *350*, 133-149.

[28] J. R. Scoville, I. A. Novicova (Cottewll Ltd.) US5900256, **1996**.

[29] B. Blaser, K. Worms, J. Schiefer, (Henkel & Cie G.m.b.H) US3122417A, **1964**.

[30] P. Wegner, (Wenger Paul C.) US20050065052A1, **2003**.

[31] R. Arrigo, M. E. Schuster, S. Abate, G. Giorgianni, G. Centi, S. Perathoner, S. Wrabetz, V. Pfeifer, M. Antonietti, R. Schlögl, *ACS Catal.* **2016**, *6*, 6959-6966.

[32] J. W. Lee, J. K. Kim, T. H. Kang, E. J. Lee, I. K. Song, *Catal. Today,* **2017**, *293-294*, 49-55.

[33] M. Seo, D. W. Lee, S. S. Han, K. Y. Lee, *ACS Catal.* **2017**, *7*, 3039-3048.

[34] Y. F. Han, J. H. Lunsford, J. H. *Catal. Lett.* **2005**, *99*, 13-19.

[35] Y. F. Han, J. H. Lunsford, *J. Catal.* **2005**, *230*, 313-316.

[36] T. Pospelova, N. Kobozev, *Russ. J. Phys. Chem.* **1961**, *35*, 1192-1197.

[37] T. A. Pospelova, N. Kobozev, *Russ. J. Phys. Chem.* **1961**, 535-542

[38] P. Landon, P. J. Collier, A. J. Papworth, C. J. Kiely, G. J. Hutchings, *Chem. Commun.* **2002**, 2058-2059.

[39] O. Mitsutaka, K. Yasutaka, Y. Kizashi, A. Tomoki, T. Susumu, H. Masatake, *Chem. Lett.* **2003**, *32*, 822-823.

[40] J. K. Edwards, B. E. Solsona, P. Landon, A. F. Carley, A. A. Herzing, M. Watanabe, C. J. Kiely, *J. Mater. Chem.* **2005**, *15*, 4595-4600.

[41] G. J. Hutchings, C. J. Kiely *Acc. Chem. Res.* **2013**, *46*, 1759-1772.

[42] A. Cybula, J. B. Priebe, M. M. Pohl, J. W. Sobczak, M. Schneider, A. Zielińska-Jurek, A. Brückner, A. Zaleska, *Appl. Catal. B,* **2014**, *152–153*, 202-211.

[43] A. Rodríguez-Gómez, F. Platero, A. Caballero, G. Colón, *Mol. Catal.* **2018**, *445*, 142-151.

[44] S. Kanungo, V. Paunovic, J. C. Schouten, M. F. Neira D'Angelo,. *Nano Lett.* **2017**, *17*, 6481-6486.

[45] R. J. Lewis, J. K. Edwards, S. J. Freakley, G. J.; Hutchings, *Ind. Eng. Chem. Res.* **2017**, *56*, 13287-13293.

[46] S. J. Freakley, R. J. Lewis, D. J. Morgan, J. K. Edwards, G. J. Hutchings, *Catal. Today,* **2015**, *248*, 10-17.

[47] A. Staykov, T. Kamachi, T. Ishihara, K. Yoshizawa, *J. Phys. Chem. C,* **2008**, *112*, 19501-19505.

[48] J. Li, T. Ishihara, K. Yoshizawa, J. *Phys. Chem. C,* **2011**, *115*, 25359-25367.

[49] J. Gu, S. Wang, Z. He, Y. Han, J. Zhang, *Catal. Sci. Technol.* **2016**, *6*, 809-817.

[50] Z. Khan, N. F. Dummer, J. K. Edwards, *Philos. Trans. R. Soc., A,* **2018**, *376*.

[51] V. R. Choudhary, C. Samanta, T. V. Choudhary, *Appl. Catal. A,* **2006**, *308*, 128-133.

[52] E. N. Ntainjua, S. J. Freakley, G. J. Hutchings, *Top. Catal.* **2012**, *55*, 718-722.

[53] T. Deguchi, H. Yamano, S. Takenouchi, M. Iwamoto, *Catal. Sci. Technol.* **2018**.

[54] Q. Liu, J. C. Bauer, R. E. Schaak, J. H.Lunsford, *Appl. Catal. A.,* **2008**, *339*, 130-136.

[55] J. Xu, L. Ouyang, G. J. Da, Q. Q. Song, X. J. Yang, Y. F. Han, *J. Catal.* **2012**, *285*, 74-82.

[56] S. Sterchele, P. Biasi, P. Centomo, P. Canton, S. Campestrini, T. Salmi, M. Zecca, *Appl. Catal. A.,* **2013**, *468*, 160-174.

[57] S. Sterchele, P. Biasi, P. Centomo, S. Campestrini, A. Shchukarev, A. R. Rautio, J. P. Mikkola, T. Salmi, M. Zecca, *Catal. Today* **2015**, *248*, 40-47.

[58] G. Bernardotto, F. Menegazzo, F. Pinna, M. Signoretto, G. Cruciani, G. Strukul, *Appl. Catal. A.,* **2009**, *358*, 129-135.

[59] S. Melada, F. Pinna, G. Strukul, S. Perathoner, G. Centi, *J. Catal.* **2006**, *237*, 213-219.

[60] S. Quon, D. Y. Jo, G. H. Han, S. S. Han, M. G.; Seo, K. Y. Lee, *J. Catal.* **2018**, *368*, 237-247.

[61] J. K. Edwards, J. Pritchard, L. Lu, M. Piccinini, G. Shaw, A. F. Carley, D. J. Morgan, C. J.; Kiely, G. J. Hutchings, *Angew. Chem. Int. Ed.* **2014**, *53*, 2381-2384.

[62] J. K. Edwards, J. Pritchard, P. J. Miedziak, M. Piccinini, A. F. Carley, Q. He, C. J. Kiely, G. J.; Hutchings, *Catal. Sci. Technol.* **2014**, *4*, 3244-3250.

[63] M. Taramasso, G. Perego, M.; B. Notari, (Snamprogetti S.p.A) US4410501, **1983**.

[64] A. Corma, *J. Catal.,* **2003**, *216*, 298-312.

[65] M. G. Clerici, *Top. Catal.,* **2001**, *15*, 257-263.

[66] W. Schuster, J. P. M. Niederer, W. F. Hoelderich, *Appl. Catal. A.,* **2001**, *209*, 131-143.

[67] G.Lv, F. Wang, X. Zhang, *Appl. Catal. A.,* **2017**, *547*, 191-198.

[68] X. Feng, X. Duan, H. Cheng, G. Qian, D. Chen, W. Yuan, X. Zhou, *J. Catal.,* **2015**, *325*, 128-135.

[69] X. Feng, X. Duan, G. Qian, X. Zhou, D. Chen, W. Yuan, *J. Catal.,* **2014**, *317*, 99-104.

[70] A. Prieto, M. Palomino, U. Díaz, A. Corma, *Appl. Catal. A.,* **2016**, *523*, 73-84.

[71] I. Moreno, N. F. Dummer, J. K. Edwards, M. Alhumaimess, M. Sankar, R. Sanz, P.; Pizarro, D. P. Serrano, G. J. Hutchings, *Catal. Sci. Technol.,* **2013**, *3*, 2425-2434.

[72] G. Li, J. K. Edwards, A. F. Carley, G. J. Hutchings, *Catal. Today* **2007**, *122*, 361-364.

[73] G. Li, J. K. Edwards, A. F. Carley, G. J. Hutchings, *Catal. Today,* **2006**, *114*, 369-371.

[74] G. Li, J. K. Edwards, A. F. Carley, G. J. Hutchings, *Catal. Commun.,* **2007**, *8*, 247-250.

[75] J. K. Edwards, B. E. Solsona, P. Landon, A. F. Carley, A. A. Herzing, C. J. Kiely, G. J. Hutchings, *J.Catal.,* **2005**, *236*, 69-79.

[76] B. E. Solsona, J. K. Edwards, P. Landon, A. F. Carley, A. A. Herzing, C. J. Kiley, G. J. Hutchings, *Chem. Mater.,* **2006**, *18*, 2689-2695.

[77] J. K. Edwards, S. F.; Parker, J. Pritchard, M. Piccinini, S. J. Freakley, Q. He, A. F. Carley, C. J. Kiely, G. J. Hutchings, *Catal. Sci. Technol.,* **2013**, *3*, 812-818.

[78] E. N. Ntainjua, J. K. Edwards, A. F. Carley, J. A. Lopez-Sanchez, J. A.; Moulijn, A. A. Herzing, C. J. Kiely, G. J.; Hutchings, *Green Chem.,* **2008**, *10*, 1162-1169.

[79] R. S. Drago, S. C. Dias, J. M. McGilvray, A. L. M. L. Mateys, *J. Phys. Chem. B*, **1998**, 102, 9, 1508-1514.

[80] L. H. Chen, X. Y. Li, G. Tian, Y. Li, J. C. Rooke, G. S. Zhu, S. L., Qiu, X. Y. Yang , B. L. Su , *Angew. Chem. Int. Ed.* **2011**, *50*, 11156-11161.

[81] G. Wu, Y. Wang, L. Wang, W; Feng, H. Shi, Y. Lin, T. Zhang, X. Jin, S. Wang, X. Wu, P. Yao, *Chem. Eng. J.* **2013**, *215-216*, 306-314.

[82] E. Duprey, P. Beaunier, M. A. Springuel-Huet, F. Bozon-Verduraz, J. Fraissard, J. M. Manoli, J. M.; Brégeault, *J. Catal.,* **1997**, *165*, 22-32.

[83] J. Pritchard, M. Piccinini, R. Tiruvalam, Q. He, N. Dimitratos, J. A. Lopez-Sanchez, D. J. Morgan, A. F. Carley, J. K. Edwards, C. J. Kiely, G. J.; Hutchings, *Catal. Sci.Technol.* **2013**, *3*, 308-317.

[84] L. Ouyang, P. Tian, G. Da, X. Xu, C. Ao, T. Chen, R. Si, J. Xu, Y. Han. *J.Catal.*, **2015**, *321*, 70-80.

[85] C. Williams, J. H. Carter, N. F. Dummer, Y. K.; Chow, D. J. Morgan, S. Yacob, P. Serna, D. J. Willock, R. J.; Meyer, S. H. Taylor, G. J. Hutchings, G. J. *ACS Catal.* **2018**, *8*, 2567-2576.

[86] D. P. Dissanayake, J. H. Lunsford, *J. Catal.,* **2002**, *206*, 173-176.

[87] M. Piccinini, E. N. Ntainjua, J. K. Edwards, A. F. Carley, J. A. Moulijn, G. J. Hutchings, *Phys. Chem. Chem. Phys.*, **2010**, 12, 2488-2492.